A molecular wire incorporating a robust hexanuclear platinum cluster†

Edmund Leary,[a] Harm Van Zalinge,[a] Simon J. Higgins,*[a] Richard J. Nichols,[a] Fabrizia Fabrizi de Biani,*[b] Piero Leoni,*[c] Lorella Marchetti[c] and Piero Zanello[b]

Reaction of $[Pt_6(CO)_4(P^tBu_2)_4Cl_2]$ with excess $HS(CH_2)_4SH$ in Et_2NH gave highly stable $[Pt_6(CO)_4(P^tBu_2)_4\{S(CH_2)_4SH\}_2]$, which adsorbs unchanged onto gold surfaces. This permitted the fabrication and electrical characterisation of gold|molecule|gold junctions involving a well-defined metal carbonyl cluster compound.

Introduction

It is well known that small metal nanoparticles have attractive size-dependent electrical properties for applications in nanoscience and nanoelectronics. They have already featured in nanoscale electrical junctions as either contacts or active elements displaying Coulomb charging.[1] Compared with nanoparticles, *molecular* metal clusters have fewer metal atoms, but have well-defined composition and structure. Although they are being considered as molecular capacitors,[2] their electrical properties are almost unexplored. As far as we know, pertinent studies are limited to the four-point probe evaluation of the resistivity of powdered samples of salts of the $[Pt_{3n}(CO)_{6n}]^{2-}$ ($n = 5$–8) cluster anions[3] and the STM assessment of the current–voltage features of samples of Pt_n or Pd_n carbonyl clusters ($n = 3$–23), on which basis their functioning as single-electron tunnelling transistors has been claimed.[4] In the latter case the junctions were fabricated by adsorbing isolated molecular clusters onto pyrolytic graphite.

Recently, a family of remarkably stable, redox-active clusters with unusual reactivity, $[Pt_6(CO)_4(P^tBu_2)_4L_2]^{x+}$, hereinafter referred to as $\{Pt_6\}L_2^{x+}$, has been described.[5–7] These have the structure indicated in Scheme 1. The dication $\{Pt_6\}(CO)_2^{2+}$ readily undergoes substitution of two terminal carbonyl ligands on the peripheral Pt atoms, to give $\{Pt_6\}L_2^{x+}$ ($x = 2$, L = *inter alia* RNC, RCN, PMe_3; $x = 0$, L = Cl [**1**], I).[7] The $\{Pt_6\}$ cluster unit is stable enough to permit the synthesis of multicluster dendrimers with σ-alkynyl spacers,[8] and alternating cluster–phenyleneethynylene oligomers,[9,10] by Cu(I)-mediated reaction of **1** with terminal alkynes. Such supramolecular metal cluster systems could be of interest in molecular-scale electronics, providing that they can be shown to be stable enough to be incorporated intact into devices.

[a] *Department of Chemistry, University of Liverpool, Crown Street, Liverpool, UK L69 7ZD. E-mail: shiggins@liv.ac.uk; Fax: +44 (0)151 794 3588; Tel: +44 (0)151 794 3512*
[b] *Dipartimento di Chimica dell'Università di Siena, Via A. Moro, 53100, Siena, Italy. E-mail: zanello@unisi.it; Fax: +39 (0)577 234254*
[c] *Dipartimento di Chimica e Chimica Industriale, Università di Pisa, Via Risorgimento 35, 56126, Pisa, Italy. E-mail: leoni@dcci.unipi.it; Fax: +39 (0)50 2219246*
† Electronic supplementary information (ESI) available: Further experimental details; STM images of **3** on gold. See DOI: 10.1039/b817424e

Scheme 1   Structures of **3** and **4**.

The possibility of using individual organic molecules for molecular-scale electronic applications has prompted the development of a number of experimental[11–15] and theoretical methods[16–18] for determining charge transport down to the single molecule level. The experimental methods include a variety of scanning probe microscopy techniques, based on either STM[14,19,20] or conducting AFM.[13,21] The scanning probe microscopy methods rely on forming molecular bridges either between a scanning probe tip and the sample surface[14,19,20] or between a probe tip and a gold nanoparticle contact.[13,22] Importantly, these techniques provide chemical attachment to the metal contacts at both ends of the molecule. Increasingly sophisticated systems, usually involving conjugated organic molecules, have been characterised in this way. Examples include molecular diodes[23–25] or switches.[19,26] A few transition metal complexes have also been examined, including redox-active examples that show the Kondo effect,[27,28] and organometallic examples.[29,30] Recently, molecules with several metal centres, either separated by conjugated spacers[28,30] or directly connected by metal–metal bonds in dinuclear derivatives or in linear extended metal atom chains (EMACs),[31–33] have been studied.

A key physical property of interest for potential device applications of metal clusters is their electron transport behaviour. In this paper, we describe the synthesis of a $\{Pt_6\}$-containing

'molecular wire', and we show that it is adsorbed intact onto Au. We then determine the electrical properties of Au|molecule|Au junctions incorporating the cluster. Compared to previous approaches of adsorbing isolated metal clusters/ nanoparticles onto self-assembled monolayers,[34] ours differs as we *initially* build the cluster into a molecular wire, and this is first fully characterised by solution spectroscopic methods.

Experimental

Preparation of $[Pt_6(\mu-P^tBu_2)_4(CO)_4\{S(CH_2)_4SH\}_2]$ (3)

1,4-Butanedithiol (94 µL, 0.801 mmol) was added to an orange solution of complex **1** (155 mg, 0.080 mmol, prepared as previously described[8]) in diethylamine (15 mL). After 24 h stirring at room temperature, all volatiles were removed *in vacuo*. The residue was extracted with toluene and filtered. Evaporation to *ca.* 2 mL and addition of *n*-hexane (10 mL) yielded a dark red solid that was separated by filtration, washed with *n*-hexane, and vacuum dried (155 mg, 92% yield). Microanalyses; found: C, 25.0; H, 4.23%. Calcd for $C_{44}H_{90}O_4P_4Pt_6S_4$: C, 25.1; H, 4.31%. UV-Vis (CH_2Cl_2 solution): 503 nm ($\varepsilon = 12.3 \times 10^3$ M^{-1} cm^{-1}), 453 nm ($\varepsilon = 9.6 \times 10^3$ M^{-1} cm^{-1}), 406 nm ($\varepsilon = 8.4 \times 10^3$ M^{-1} cm^{-1}), 295 nm ($\varepsilon = 40 \times 10^3$ M^{-1} cm^{-1}). IR (solid state): 2501 (ν_{SH}), 2004 cm^{-1} (ν_{CO}). ^1H NMR (C_6D_6, ppm; symbol # used to label ^1H, ^{13}C, and ^{31}P peaks with ^{195}Pt satellites, *J* Hz): δ = 3.33# (t, $^3J_{HPt}$ 39.7, $^3J_{HH}$ 7.0, 2H, PtSC*H*$_2$), (dt, $^3J_{HH}$ 7.0, 8.0, 2H, C*H*$_2$SH), 1.85 (m, 4H, C*H*$_2$), 1.50 (vt, $|^3J_{HP} + {}^5J_{HP}|$ 7.6, 36H, CC*H*$_3$), 1.14 (t, 1H, $^3J_{HH}$ 8.0, S*H*). $^{13}C\{^1H\}$ NMR (C_6D_6): 213.9 (s, *C*O), 43.9 (s, *C*CH$_3$), 39.9 (t, $^3J_{CP}$ 6, PtS*C*H$_2$), 36.0# (s, $^3J_{CPt}$ 68, PtSCH$_2$*C*H$_2$), 34.2 (s, *C*H$_2$), 31.6 (s, *C*H$_3$), 24.9 (s, *C*H$_2$SH). $^{31}P\{^1H\}$ NMR (CDCl$_3$): 320.1# (s). $^{195}Pt\{^1H\}$ NMR (CDCl$_3$): −4626 (1Pt), −3069 (2Pt).

Preparation of $[Pt_6(\mu-P^tBu_2)_4(CO)_4(SCN)_2]$ (4)

A solution of KSCN (10 mg, 0.103 mmol) in H$_2$O (2 mL) was added to a solution of $[\{Pt_6\}(CO)_2](CF_3SO_3)_2$[5] (74 mg, 0.0334 mmol) in acetone (5 mL) with constant stirring at 25 °C. An orange solid precipitated out quickly and the solution was stirred further for *ca.* 15 min. The product was filtered off, washed with water–acetone (1 : 1) and vacuum dried (microcrystalline orange solid, 56 mg, 85% yield). Microanalyses; found: C, 23.0; H, 3.48; N, 1.42%. Calcd for $C_{38}H_{72}N_2O_4P_4Pt_6S_2$: C, 23.1; H, 3.67; N, 1.41%. ^1H NMR (CDCl$_3$, 25 °C): δ (ppm) = 1.52 (vt, $^3J_{HP} + {}^5J_{HP}$ = 7.6 Hz, CC*H*$_3$). $^{13}C\{^1H\}$ NMR (CDCl$_3$, 25 °C): δ (ppm) = 207.1 (s, *C*O), 121.6 (s, *C*N), 45.2 (m, *C*CH$_3$), 31.7 (s, *C*H$_3$). $^{31}P\{^1H\}$ NMR (CDCl$_3$, 25 °C): δ (ppm) = 331.1# (s) $^{195}Pt\{^1H\}$ NMR (CDCl$_3$, 25 °C): δ (ppm) = −4553 (m, 1 Pt), −3284 (m, 2 Pt). IR (solid state): = 2116, 2080 (ν_{CN}), 2014 cm^{-1} (ν_{CO}).

Experimental details for PM-IRRAS and XPS experiments

XPS spectra were acquired using a Scienta ESCA 300 spectrometer (NCESS, Daresbury Laboratory, UK) at 90° and 10° take-off angles; we present the 10° angle data here. The spectra were referenced to the Au 4d 5/2 line positioned at 335.0 eV. The molecule **3** was adsorbed onto a gold-on-glass substrate from a 1×10^{-4} M dry CH$_2$Cl$_2$ solution. The adsorption time was 3 min. The gold substrate was flame-annealed in a butane flame just prior to adsorption.

I(s) single molecule conductance determinations

I(s) experiments were conducted as previously outlined for organic dithiols.[19,35–37] Briefly, a low-coverage monolayer was deposited onto Au on glass slides as above, except that the adsorption time was 1 min. A gold STM tip was brought to a fixed distance above a monolayer-modified gold surface under argon, controlled using the set point current. The feedback loop was switched off, the tip was withdrawn while maintaining a constant *x–y* position, and a current–distance (*I(s)*, where *I* is the current and *s* = relative tip–sample distance) curve was collected. Direct contact between tip and substrate is avoided, and Au|molecule|Au junctions form spontaneously under these conditions as long as the tip is close enough to the surface. We typically observed current–distance behaviour characteristic of the formation of molecular wires (Fig. 2a) with a plateau in the current (*I(w)*) due to conductance through the fully-extended molecule. As the tip was withdrawn further, the molecule detached at a distance characteristic of its length (tunnelling current therefore diminishing sharply), and this break-off distance was also measured. The experiment was repeated many times, and the results were analysed statistically, using conductance (*G*) histograms in which the complete current–distance (*I(s)*) curves are taken into the analysis, as in Fig. 2b.

Results and discussion

Synthesis and characterisation of 3 and 4

Treatment of $\{Pt_6\}Cl_2$ with excess 1,4-butanedithiol gave $\{Pt_6\}[S(CH_2)_4SH]_2$ (**3**) as shown in Scheme 1,† and treatment of the labile $[\{Pt_6\}(CO)_2](CF_3SO_3)_2$[5] with KSCN in acetone gave complex **4**. Significant IR and NMR parameters for **3** and **4** (see Experimental) compare well with corresponding data for analogous derivatives characterized by X-ray diffraction.[7] These data, together with satisfactory micro-analyses, support the structures shown in Scheme 1. As expected on the basis of the general redox behaviour of the family of clusters $\{Pt_6\}X_2$,[7] compound **3** undergoes a chemically-reversible one-electron reduction at $E° = -1.49$ V, and a second, less reversible reduction at -1.64 V *vs.* saturated calomel electrode (SCE; CH$_2$Cl$_2$, 0.2 M Bu$_4$NPF$_6$; Pt, Au or ITO working electrode). Two irreversible oxidations ($E_P^A = +0.58$ and $+0.75$ V; the one-electron oxidation of ferrocene occurred at $+0.39$ V under these conditions) are also apparent. The voltammograms did not vary significantly with the identity of the working electrode, and the peak currents scaled linearly with the square root of scan rate, suggesting that adsorption is insignificant under these conditions. The electronic spectrum shows several intense bands in the visible region. The lowest-energy band is at 503 nm (2.46 eV). These data indicate that although the $\{Pt_6\}$ cluster frontier orbitals are certainly closer in energy to the Fermi energy of gold contacts (see below) than are the frontier orbitals of the alkyl 'spacers', both the oxidation and reduction waves are outside

the voltage 'window' accessible with Au–S contacts. Complex **4** shows ν_{CN} modes consistent with S-bound thiocyanate[38] in its infrared spectrum.

Adsorption of 3 onto Au

We wished to employ the scanning tunnelling microscopy (STM)-based $I(s)$ technique of Haiss *et al.*[19] to fabricate Au|**3**|Au molecular junctions and to measure their electrical properties. It was therefore first necessary to investigate whether **3** could be adsorbed intact onto Au surfaces. A gold-coated glass slide was flame-annealed to produce a Au(111) texture,[39] then dipped into a dilute (10^{-4}–10^{-5} M) solution of **3** in dry CH_2Cl_2 for 1 min to allow the formation of a low-coverage monolayer (3 min adsorption time for XPS). The adsorbed complex was characterised by X-ray photoelectron (XPS) and polarisation modulated infrared reflection absorption (PM-IRRAS) spectroscopies, and scanning tunnelling microscopy (STM) imaging. Complex **3** shows a single, rather broad, CO stretching band at 2004 cm^{-1} in the solid state (2009 cm^{-1} in CH_2Cl_2 solution). The PM-IRRAS spectrum of the monolayer shows an intense band at 2014 cm^{-1} (Fig. 1a). The XPS spectrum shows Pt $4f_{5/2}$ and $4f_{7/2}$ peaks at 76.1 and 72.8 eV, respectively (Fig. 1b). The $4f_{7/2}$ peak position is similar to those of related Pt–Pt bonded species, such as $[Pt_3(\mu^3\text{-}CO)(\mu\text{-}dppm)_3]^{2+}$ (dppm = $Ph_2PCH_2PPh_2$; 72.9 eV) or $[Pt_2Cl_2(\mu\text{-}dppm)_2]$ (72.4 eV[40]), and is notably different from Pt metal (70.9 eV[41]). In addition, peaks due to carbon, sulfur and phosphorus were seen, in the expected intensity ratios, consistent with the molecule being adsorbed to the surface intact. In STM images of the low-coverage monolayer (Fig. S1, ESI†), the molecules showed up as bright dots, and line scans across these dots showed that their height is consistent with intact **3**, although a quantitative comparison cannot be drawn from the STM height measurements since STM probes the density of electronic states rather than the physical height.

Single molecule conductance measurements on 3

With evidence in hand that **3** adsorbs intact onto Au under these conditions, we fabricated and measured the electrical properties of Au|**3**|Au single molecule junctions using the $I(s)$ technique.

Fig. 2a shows some typical current–distance curves obtained for **3**, and Fig. 2b shows a histogram constructed by co-adding all $I(s)$ curves. The conductance determined for Au|**3**|Au single
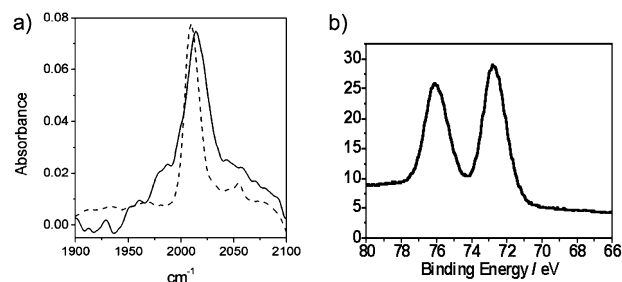
molecule junctions is (2.4 ± 0.5) nS, measured under argon at $+0.2$ V bias (Table 1). It is important to note that the $I(s)$ technique provides good evidence that we are indeed measuring intact molecules of **3** in these junctions, making contact *via* the terminal thiols, because the mean break-off distance (Fig. 2c) is consistent with the full (terminal thiol S···S) length of the molecules (2.4 nm for the fully-extended, transoid conformer of **3** as determined by molecular mechanics). The degree of uncertainty in the detachment distance measurement is larger than in the determination of conductance because of the range of contact geometries, and the difficulty of maintaining a constant starting-point in the measurements.

As a control experiment, we determined the conductance of Au|1,8-octanedithiol|Au junctions under conditions identical to those for **3**, *i.e.* under an argon atmosphere and with a similar set point current (Fig. 3). The S···S distance for 1,8-octanedithiol is 1.19 nm, much shorter than **3**, and the conductance value measured was 3.7 ± 0.9 nS ($+0.6$ V bias). It is now clear that several conductance values for Au|1,n-alkane-dithiol|Au junction are observable experimentally (see, for
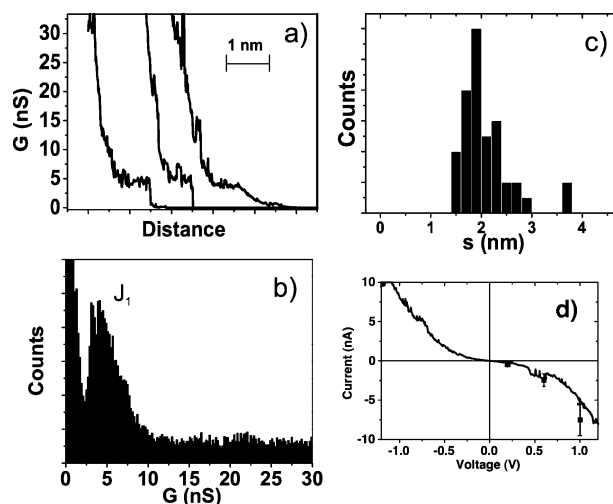

Fig. 2 (a) Example current–distance relations for several $I(s)$ determinations on **3**. (b) Histogram of all the curves showing current plateaux ($I(w)$) observed for **3** (set point current $I(w)$ = 20 nA, tip–sample bias $+0.6$ V). (c) Histogram of the wire break-off distance (s_W) with initial distance (s_0) added. (d) Representative experiment in which a Au tip is scanned between ±1.5 V while held above the surface of a monolayer of **3** on a Au substrate, and a molecule (or molecules) bridge(s) the substrate and tip for the whole of the scan. Other experiments are shown (superimposed) in Fig. S2 (ESI†); only one example is shown here for clarity. The mean currents obtained from the results of multiple $I(s)$ experiments at different tip potentials are shown as black squares with standard deviations.

Table 1

Compound	Length (S···S separation)/nm	Single molecule conductance of lowest conductance group/nS
3	2.4	2.4 ± 0.5
Octanedithiol	1.19	3.7 ± 0.9
Octadecanedithiol[a]	2.45	4.6×10^{-5}

[a] Single molecule conductance obtained by extrapolation; see text.

Fig. 1 (a) PM-IRRAS spectrum of compound **3** on Au (111) substrate (solid line) and solution IR spectrum (dash line). (b) XPS spectrum of the Pt 4f region of **3** on Au (111).
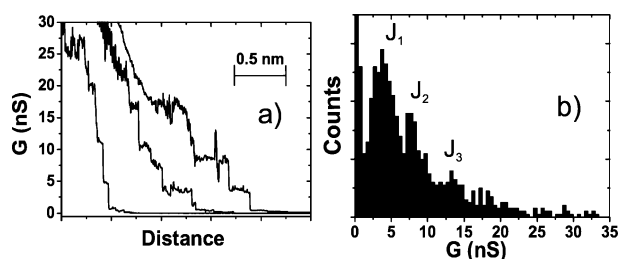
Fig. 3 (a) Example current–distance relations for several $I(s)$ determinations on octanedithiol; experiments conducted under dry argon. (b) Histogram of 250 current plateaux observed for octanedithiol under argon (set point current $I(w) = 20$ nA, tip–sample bias 0.6 V). J_n refers to different peaks due to n molecules in the junctions.

Fig. 4 (a) Typical $I(s)$ curves for molecule **4** (bias $+0.1$ V, $I(w) = 50$ nA). (b) Plot of $I(s)$ histogram peak currents for measurements on **4** plotted against bias potential. Error bars from width of histogram peaks at half maxima.

example, ref. 42–44). We, and others, have recently found that the value depends upon the degree of surface roughness.[44,45] Under the conditions employed in this study for **3**, i.e. a dry Ar atmosphere, we find that 1,n-alkanedithiols give conductance values in agreement with the Xu and Tao break junction method 'low' conductance values (for 1,8-octanedithiol, 3.9 nS[42]). For comparison the conductance of compound **3** is shown alongside that of octanedithiol and octadecanedithiol in Table 1. The lengths of the respective molecules (from molecular mechanics) are also included.

Au|1,n-alkanedithiol|Au junctions have been extensively investigated. They conduct by superexchange, so the conductance, G, depends exponentially on the number of repeat units in the wire, n, giving the dependence $G = A\exp(-\beta_N n)$, where β_N is a measure of electron attenuation per n. The S$\cdots$S distance in **3** of 2.4 nm is roughly equivalent to that of $HS(CH_2)_{18}SH$ (S$\cdots$S = 2.45 nm). The single molecule conductance of $HS(CH_2)_{18}SH$ at the same bias would be too small to measure, but it can be estimated by extrapolation from published data on $HS(CH_2)_nSH$ ($n = 6, 8, 10$)[46] using the above relation as 4.6×10^{-5} nS. Thus, length for length, the $\{Pt_6\}$ cluster is markedly more conductive than an alkyl chain, showing that the cluster plays a determining role in transport across this molecular bridge. The current–voltage behaviour of **3** was also investigated by carrying out $I(s)$ measurements at different bias voltages ($+0.2$, $+0.6$ and $+1.0$ V), and additionally by scanning the bias potential with molecule(s) present in the gap (Fig. 2d). Attempts to fit the observed nonlinear I–V behaviour to a simple Simmons model, as used successfully for alkanedithiols,[47] were unsuccessful, but this model is probably inappropriate for **3**, because the molecule is effectively a double tunnelling barrier with the $\{Pt_6\}$ unit acting as a 'well'.

We have used the $I(s)$ technique to determine the single molecule conductance of molecules containing either organic redox-active groups, or simple aromatic units, sandwiched between alkanethiol 'spacers'. These include viologen,[19] pyrrolo tetrathiafulvalene[48] and benzene[37] derivatives. When contacted to gold electrodes via the thiol groups, these can be regarded as the single molecule equivalents of inorganic double tunnelling barrier junctions, as the frontier orbital energies for the alkyl 'spacers' lie far from the gold
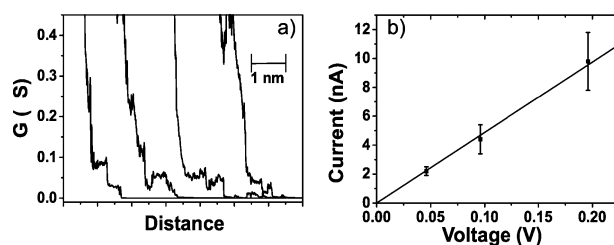
Fermi energy (E_F), while the frontier orbitals of the π-system (barrier indentation) are much closer in energy. As a result, the conductance of Au|molecule|Au junctions is very much greater for such molecules than for an alkanedithiol of equivalent length. The electrochemical and electronic spectroscopic data show that the frontier orbitals of the $\{Pt_6\}$ cluster core are similarly much closer in energy to the gold E_F than the alkyl linkers, although they lie outside the range where they can be electrochemically addressed within the potential region where Au–S bonds are stable. The conductance of **3** is consistent with the $\{Pt_6\}$ unit behaving in a similar fashion to the previously studied benzene ring-containing compounds.[37,48]

$I(s)$ measurements on [Pt$_6$(μ-P^{t}Bu$_2$)$_4$(CO)$_4$(SCN)$_2$] (4)

Further (indirect) evidence that we are indeed measuring the conductance through the terminal thiol groups of **3** was obtained by measuring the conductance of Au|molecule|Au junctions involving [Pt$_6$(μ-P^{t}Bu$_2$)$_4$(CO)$_4$(SCN)$_2$] (**4**).[5] $I(s)$ data on **4** (at $+0.05$, $+0.1$ and $+0.2$ V bias) showed a linear current–voltage relation in this bias range within experimental error. From the slope of the plot (Fig. 4), we calculate a conductance of 50 nS for **4**, approximately 20 times higher than for **3**, as expected since the alkyl spacer groups, with their higher HOMO–LUMO separation, are absent in **4**. It is possible that contact is made via the sulfur atom in these experiments, since thiocyanates are known to undergo C–S cleavage on Au as a result of the strong affinity of both the resulting RS^- and CN^- for Au.[49]

Conclusions

We have demonstrated that (i) the particularly robust metal carbonyl cluster unit $\{Pt_6\}$ in **3** can be adsorbed unchanged on a Au surface, and that (ii) the electronic properties of single molecules incorporating this cluster can be determined using the $I(s)$ technique. The $\{Pt_6\}$ unit behaves in an analogous way to previously studied conjugated organic groups. Future work will involve the use of conjugated 'linkers', such as aryl alkynes, to contact the cluster, and the investigation of aryl alkyne-linked oligomers containing more than one cluster unit. In the future, it may also be possible to incorporate larger clusters within similar defined metal–organic frameworks, where single-electron charging events can be accessed within the bias window where the contacts are stable.

Acknowledgements

Notes and references

1 N. Oncel, A. S. Hallback, H. J. W. Zandvliet, E. A. Speets, B. J. Ravoo, D. N. Reinhoudt and B. Poelsema, *J. Chem. Phys.*, 2005, **123**, 044703.

2 C. Femoni, M. C. Iapalucci, G. Longoni, P. H. Svensson, P. Zanello and F. F. De Biani, *Chem.–Eur. J.*, 2004, **10**, 2318–2326.

3 C. Femoni, F. Kaswalder, M. C. Iapalucci, G. Longoni and S. Zacchini, *Eur. J. Inorg. Chem.*, 2007, 1483–1486.

4 S. P. Gubin, Y. V. Gulayev, G. B. Khomutov, V. V. Kislov, V. V. Kolesov, E. S. Soldatov and K. S. Sulaimankulov, *Nanotechnology*, 2002, **13**, 185–194.

5 P. Leoni, F. Marchetti, L. Marchetti, M. Pasquali and S. Quaglierini, *Angew. Chem., Int. Ed.*, 2001, **40**, 3617–3618.

6 F. F. de Biani, A. Ienco, F. Laschi, P. Leoni, F. Marchetti, L. Marchetti, C. Mealli and P. Zanello, *J. Am. Chem. Soc.*, 2005, **127**, 3076–3089.

7 C. Bonaccorsi, F. F. de Biani, P. Leoni, F. Marchetti, L. Marchetti and P. Zanello, *Chem.–Eur. J.*, 2008, **14**, 847–856.

8 A. Albinati, P. Leoni, L. Marchetti and S. Rizzato, *Angew. Chem., Int. Ed.*, 2003, **42**, 5990–5993.

9 P. Leoni, F. Marchetti, L. Marchetti and M. Pasquali, *Chem. Commun.*, 2003, 2372–2373.

10 P. Leoni, L. Marchetti, S. K. Mohapatra, G. Ruggeri and L. Ricci, *Organometallics*, 2006, **25**, 4226–4230.

11 M. A. Reed, C. Zhou, C. J. Muller, T. P. Burgin and J. M. Tour, *Science*, 1997, **278**, 252–254.

12 D. Porath, A. Bezryadin, S. des Vries and C. N. Dekker, *Nature*, 2000, **403**, 635–638.

13 X. D. Cui, A. Primak, J. Tomfohr, O. F. Sankey, A. L. Moore, T. A. Moore, D. Gust, G. Harris and S. M. Lindsay, *Science*, 2001, **294**, 571–574.

14 B. Q. Xu and N. J. Tao, *Science*, 2003, **301**, 1221–1223.

15 T. Dadosh, Y. Gordin, R. Kranhe, I. Khivrich, D. Mahalu, V. Frydman, J. Sperling, A. Yacoby and I. Bar-Joseph, *Nature*, 2005, **436**, 677–680.

16 M. Brandbyge, J. L. Mozos, P. Ordejon, J. Taylor and K. Stokbro, *Phys. Rev. B: Condens. Matter*, 2002, **65**, 165401.

17 Y. Fujimoto and K. Hirose, *Phys. Rev. B: Condens. Matter*, 2003, **67**, 195315.

18 A. R. Rocha, V. M. Garcia-Suarez, S. Bailey, C. Lambert, J. Ferrer and S. Sanvito, *Phys. Rev. B: Condens. Matter*, 2006, **73**, 085414.

19 W. Haiss, H. van Zalinge, S. J. Higgins, D. Bethell, H. Höbenreich, D. J. Schiffrin and R. J. Nichols, *J. Am. Chem. Soc.*, 2003, **125**, 15294–15295.

20 W. Haiss, R. J. Nichols, H. van Zalinge, S. J. Higgins, D. Bethell and D. J. Schiffrin, *Phys. Chem. Chem. Phys.*, 2004, **6**, 4330–4337.

21 G. Leatherman, E. N. Durantini, D. Gust, T. A. Moore, A. L. Moore, S. Stone, Z. Zhou, P. Rez, Y. Z. Liu and S. M. Lindsay, *J. Phys. Chem. B*, 1999, **103**, 4006–4010.

22 T. Morita and S. Lindsay, *J. Am. Chem. Soc.*, 2007, **128**, 7262–7263.

23 P. Jiang, G. M. Morales, W. You and L. Yu, *Angew. Chem., Int. Ed.*, 2004, **43**, 4471–4475.

24 G. M. Morales, P. Jiang, S. Yuan, Y. Lee, A. Sanchez, W. You and L. Yu, *J. Am. Chem. Soc.*, 2005, **127**, 10456–10457.

25 M. Elbing, R. Ochs, M. Koentopp, M. Fischer, C. von Hanisch, F. Weigend, F. Evers, H. B. Weber and M. Mayor, *Proc. Natl. Acad. Sci. U. S. A.*, 2005, **102**, 8815–8820.

26 E. Lörtscher, J. W. Ciszek, J. Tour and H. Riel, *Small*, 2006, **2**, 973–977.

27 M. Mayor, C. von Hänisch, H. B. Weber, J. Reichert and D. Beckman, *Angew. Chem., Int. Ed.*, 2002, **41**, 1183–1186.

28 W. J. Liang, M. P. Shores, M. Bockrath, J. R. Long and H. K. Park, *Nature*, 2002, **417**, 725–729.

29 T. L. Schull, J. G. Kushmerick, C. H. Patterson, C. George, M. H. Moore, S. K. Pollack and R. Shashidhar, *J. Am. Chem. Soc.*, 2003, **125**, 3202–3203.

30 B. S. Kim, J. M. Beebe, C. Olivier, S. Rigaut, D. Touchard, J. G. Kushmerick, X. Y. Zhu and C. D. Frisbie, *J. Phys. Chem. C*, 2007, **111**, 7521–7526.

31 I. W. P. Chen, M. D. Fu, W. H. Tseng, J. Y. Yu, S. H. Wu, C. J. Ku, C. H. Chen and S. M. Peng, *Angew. Chem., Int. Ed.*, 2006, **45**, 5814–5818.

32 D. H. Chae, J. F. Berry, S. Jung, F. A. Cotton, C. A. Murillo and Z. Yao, *Nano Lett.*, 2006, **6**, 165–168.

33 A. S. Blum, T. Ren, D. A. Parish, S. A. Trammell, M. H. Moore, J. G. Kushmerick, G. L. Xu, J. R. Deschamps, S. K. Pollack and R. Shashidhar, *J. Am. Chem. Soc.*, 2005, **127**, 10010–10011.

34 P. S. Jensen, Q. Chi, F. B. Grumsen, J. M. Abad, A. Horsewell, D. J. Schiffrin and J. Ulstrup, *J. Phys. Chem. C*, 2007, **111**, 6124–6132.

35 W. Haiss, H. v. Zalinge, H. Höbenreich, D. Bethell, D. J. Schiffrin, S. J. Higgins and R. J. Nichols, *Langmuir*, 2004, **20**, 7694–7702.

36 W. Haiss, C. S. Wang, I. Grace, A. S. Batsanov, D. J. Schiffrin, S. J. Higgins, M. R. Bryce, C. J. Lambert and R. J. Nichols, *Nat. Mater.*, 2006, **5**, 995–1002.

37 E. Leary, S. J. Higgins, H. van Zalinge, W. Haiss and R. J. Nichols, *Chem. Commun.*, 2007, 3939–3942.

38 R. A. Bailey, S. L. Kozak, T. W. Michelsen and W. N. Mills, *Coord. Chem. Rev.*, 1971, **6**, 407.

39 W. Haiss, D. Lackey, J. K. Sass and K. H. Besocke, *J. Chem. Phys.*, 1991, **95**, 2193–2196.

40 M. C. Jennings, G. Schoettel, S. Roy, R. J. Puddephatt, G. Douglas, L. Manojlovic-Muir and K. W. Muir, *Organometallics*, 1991, **10**, 580–586.

41 B. C. Beard and P. N. Ross, *J. Phys. Chem.*, 1986, **90**, 6811–6817.

42 F. Chen, X. L. Li, J. Hihath, Z. F. Huang and N. J. Tao, *J. Am. Chem. Soc.*, 2006, **128**, 15874–15881.

43 A. Nishikawa, J. Tobita, Y. Kato, S. Fujii, M. Suzuki and M. Fujihara, *Nanotechnology*, 2007, **18**, 424005.

44 C. Li, I. Pobelov, T. Wandlowski, A. Bagrets, A. Arnold and F. Evers, *J. Am. Chem. Soc.*, 2008, **130**, 318–326.

45 W. Haiss, S. Martín, E. Leary, H. van Zalinge, S. J. Higgins, L. Bouffier and R. J. Nichols, *J. Phys. Chem. C*, 2009, DOI: 10.1021/jp811142d.

46 X. L. Li, J. He, J. Hihath, B. Q. Xu, S. M. Lindsay and N. J. Tao, *J. Am. Chem. Soc.*, 2006, **128**, 2135–2141.

47 W. Wang, T. R. Lee and M. A. Reed, *Rep. Prog. Phys.*, 2005, **68**, 523–544.

48 E. Leary, S. J. Higgins, H. van Zalinge, W. Haiss, R. J. Nichols, S. Nygaard, J. O. Jeppesen and J. Ulstrup, *J. Am. Chem. Soc.*, 2008, **130**, 12204–12205.

49 J. W. Ciszek, M. P. Stewart and J. M. Tour, *J. Am. Chem. Soc.*, 2004, **126**, 13172–13173.